'94 대한전기학회 추계학술대회 논문집(1994. 11. 18)

TWO DIMENSIONAL NUMERICAL SIMULATION PROGRAM FOR HYDROGENATED AMORPHOUS SILICON THIN FILM TRANSISTORS

Jong S. Choi° and Gerold W. Neudeck*

° Department of Electronic, Electrical and Control Engineering,
Hong-Ik University, South Korea
* School of Electrical Engineering, Purdue University
U.S.A.

Abstract

A non-uniform finite-difference Thin Film Transistor Simulation Program (TFTSP) has been developed for hydrogenated amorphous silicon TFTs. TFTSP was developed to remove as many of simplifying assumptions as possible and to provide flexibility in the modeling of TFTs so that different model assumptions may be analyzed and compared. In order to insure its usefulness and versatility as an analytic and design tool it is important for the code to satisfy a number of conditions. However, at the beginning stage of the program development, this paper shows that the code can compute the static terminal characteristics of a-Si:H TFTs under a wide range of bias conditions to allow for comparison of the model with experiment. Some of those comparisons include transfer characteristics and I-V characteristics. TFTSP will be refined to conveniently model the performances of TFTs of different designs and to analyze many anomalous behaviors and factors of a-Si:H TFTs.

I. Introduction

Hydrogenated Amorphous Silicon (a-Si:H) Thin Film Transistors (TFTs) have been under research for the past thirty years, but it is only in the last decade that an explosive growth has occured in this field. Advances made in office automation and consumer electronics have stimulated increasing research activities directed at the development of a new generation input/output devices. Although a-Si:H TFT has been under intensive study in the last decade, there is much room both for further understanding of the fundamental device physics and for improvement of device technologies. At this stage of development of a-Si:H TFTs, two-dimensional (2-D) device simulation becomes very helpful in that it would help explain the various experimental results and also to get insight of the device physics. Based on the 2-D simulation results, further improvement of the existing structure and the possible design of new TFT structure can then be made.

Recently, several 2-D computer simulations for a-Si:H TFTs [1],[2],[3] have been reported. However, many simplifying assumptions were made in these models which may have limited the accuracy of their results. A 2-D computer simulation code, Thin Film Transistor Simulation Program (TFTSP) for a-Si:H TFTs, was developed to remove as many of these simplifying assumptions as possible and to provide flexibility in the modeling of TFTs so that different model assumptions may be analyzed and compared. Because the physical parameters describing a-Si:H are not well known, TFTSP was developed to allow considerable flexibility in the choice of these parameters so that the implications of these choices can be fully investigated.

II. The Steady-State Equations for a-Si:H

a-Si:H can be modeled by assuming that the bands possess mobility edges which can be treated as a conduction band edge (E_C) and as a valence band edge (E_V), defining a mobility gap. Electrons higher in energy than E_C and holes lower in energy than E_V are treated as mobile carriers. This argument allows a-Si:H devices to

be modeled by the usual set of drift-diffusion equations. However, when modeling amorphous silicon devices, it is very important to account for the high concentration of trapped charge in the continuous distribution of localized states in the mobility gap. Electrons and holes in the band tails and the dangling-bond defect states do not contribute to the conduction process at room temperature. Electrons trapped by localized states dominate the potential distribution in the active a-Si region and thus influence the performance of a-Si devices. Thus, the situation is considerablely more complicated than the one encountered when modeling crystalline semiconductor devices in which discrete energies for dopants and recombination centers can be assumed. In a-Si:H, these must be modeled by a continum of states. The computer simulation for a-Si:H devices is therefore based on the solution to the following set of partial differential equations under steady-state conditions:

$$\nabla^2 V = \frac{q}{\varepsilon}(p - n + N_{GAP} + N_D^+ - N_A^-) \quad (1)$$

$$\nabla \cdot \mathbf{J}_n = q \cdot (R_n - G_n) \quad (2)$$

$$\nabla \cdot \mathbf{J}_p = -q \cdot (R_p - G_p) \quad (3)$$

For homo-structures, the hole and electron currents are given by the following transport equations:

$$\mathbf{J}_n = kT\mu_n \cdot \nabla n - q\mu_n n \cdot \nabla V, \quad (4)$$

$$\mathbf{J}_p = -kT\mu_p \cdot \nabla p - q\mu_p p \cdot \nabla V. \quad (5)$$

In these equations, all the terms have their usual definitions except N_{GAP} which accounts for the charge trapped in the exponential tail states (indicated by subscript tail) and the dangling-bond defect states (indicated by subscript db):

$$N_{GAP} = N_{tail} + N_{db}. \quad (6)$$

The total recombination due to these mechanism is

$$R - G = (R - G)_{tail} + (R - G)_{db}. \quad (7)$$

Recombination through the donor and acceptor impurity states is neglected, as is band-to-band recombination. Vectors are denoted here as boldface. In Poisson's equation, it was assumed that the dielectric constant does not vary with position. The electron and hole mobilities are the band mobilities. The ideal case, in which insulator has infinite resistivity and no fixed charge, was postulated.

III. Physical Models and Boundary Conditions

The important terms in the equations (1) to (7) are briefly summarized below. Most of models have been suggested and extended for a-Si:H device simulations by Gray [4] and Park [5]. The detailed treatment can be found in references [4] and [5].

Due to its amorphous nature it may be necessary to model the donor and acceptor states in amorphous silicon as a Gaussian distribution of levels about a central energy, E_D and E_A, respectively. It is assumed that these states do not act as recombination centers and this formulation results in the quasi-Fermi levels for electrons and holes determine the occupation of the donor and acceptor levels, respectively. The energy distribution of the band tails has an exponential energy dependence which begins some distance away from the mobility edges [6], [7]. The valence band tail and the conduction band tail are assumed to be donor-like and acceptor-like, respectively. The theory of Taylor and Simmons [8] for arbitrary distributions of trapping levels is applied to calculate the net trapped charge in the band tails, N_{GAP}.

Dangling-bond defect states are located near the middle of the mobility gap and play an important role in the operation of a-Si:H devices. These are distributed states which are amphoteric in nature. The distribution is assumed to be Gaussian. There are three possible charge states for dangling-bond stsates: positive (D^+), neutral (D^o), and negative (D^-). The density of these states is referred to as N_{D^+}, N_{D^o}, and N_{D^-}, respectively. Trapping and recombination statistics for multiple energy-level defect states has been treated by Sah [9], and by Sah and Shockley [10]. This treatment has been extended for a Gaussian distribution of such states by Gray [4] and Park [5]. The rate of recombination via these states is also given

The program, TFT2SP contains two types of basic boundary conditions: simple Dirichlet (ohmic contact) and Neumann (reflective) boundary conditions. These contact types are indicated in Figure 1 for all the boundaries of the simulated TFT structure. The insulating contact between metal gate and gate insulator is also treated as an ohmic contact. Along the outer (non-contacted) edges and at the interface between two different materials of the device to be simulated, the difference between the normalized components of the respective electric displacements must be equal to any surface charge density, ρ_{ss}, present along the interface. Current is not permitted to flow from the semiconductor into an insulating region and current densities at interface are

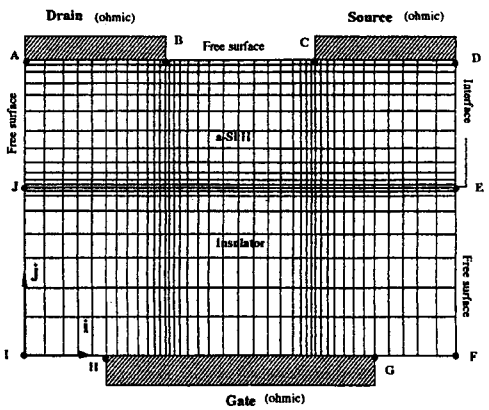

Figure 1 Two-dimensional finite difference grid for an a-Si:H TFT with boundary surface types.

controlled by recombination at the interface.

IV. Program Description

The highly non-linear nature of the transport equations to be solved suggests the use of approximate numerical methods. For simplicity and accuracy, the well-known non-uniform finite difference method of the first and second derivatives with respect to the position is chosen to discretize Poisson's equation and the hole and electron continuity equations [11], [12]. A schematic two-dimensional finite difference grid, the concept of which is implicit to the choice of a difference method, is illustrated in Figure 1. The drift-diffusion transport equations were discretized using Scharfetter-Gummel method [13]. The discretized equations were normalized by the scheme of A. de Mari [14] except that the signs of currents are conventional. For the discretization at a-Si:H/SiN_x interface nodes, the algorithm, devised by Sutherland [15], was employed for the explicit inclusion of interface surface charge in the finite-difference equations.

Since the band tails fall off rapidly, away from the band edges, the integrals representing the charge or recombination rate of the band tails can be well approximated by the following sum [4]:

$$I = \int_0^\infty f(z)e^{-z}dz = \sum_{i=1}^{n} w_i f(z_i) \qquad (8)$$

where w_i and z_i are the weight factors and zeros of one of the Laguerre polynomials. This approximation is commonly referred to as Laguerre integration. For the remaining integrals of state functions which have a Gaussian shape, if the Gaussians are not overly broad, another approximation, Hermite integration, can be applied [4]:

$$I = \int_{-\infty}^{\infty} f(z)e^{-z^2}dz = \sum_{i=1}^{n} w_i f(z_i), \qquad (9)$$

where, in this case, w_i and z_i are the weight factors and zeros of one of the Hermite polynomials. These integral approximations considerably reduce the computation time without appreciably affecting the accuracy [4]. A 15-point Laguerre and a 9-point Hermite integration have been implemented. When the bias applied to electrodes are abruptly changed by large steps, it is usually necessary to damp numerical ringing in the Newton iterations. The numerical damping algorithm presented by Brown and Lindsay [16] was used.

VI. Model Verification

In order to gain confidence in any numerical model, it is necessary to examine some test cases for which either an approximate analytical solution or experimentally measured data is available. In this section the simulated results for a specific TFT are presented and compared to the measured data. An a-Si:H TFT with SiO_2 gate insulator was simulated for n-type device. The simplified structure of an a-Si:H TFT as shown in Figure 1 was simulated for the verification of the model. The important material and device parameters which were optimized to have the best fit to the experimental data and used in the computation are summarized in Table 1 and 2. The set of parameters used here may be not a unique one. However, they are in the reasonable range. The relative importance of the different sources of recombination depends entirely on the choice of capture cross sections involved, and parameters used here are not necessarily the correct ones but optimized through the photoconductivity study of a-Si:H solar cell [5]. A schematic energy band model for the gap states is shown in Figure 2. Although the program was written so that surface states charge can be included, their effect on the solution is quite small and can be accounted for within the flatband voltage and/or other gap states, hence they were neglected for the present simulations. The effective values of the electron and hole band mobilities were optimized as constants for the best fit to the experimental results. The distribution of electrostatic potential and free electron concentration under the bias condition of V_G=5 V, V_D=9.6 V, and V_S= 0 V is

assumptions as possible. Especially, recombination due to the exponential band-tail states and the amphoteric dangling-bond defect states as well as hole current are incorporated in the program. This computer program was employed to verify its validity by simulating the current-voltage characteristics of an a-Si:H TFT. The simulated results show good agreement with the experimental data indicating that this computer simulations are realistic. Although it is possible that other sets of physical

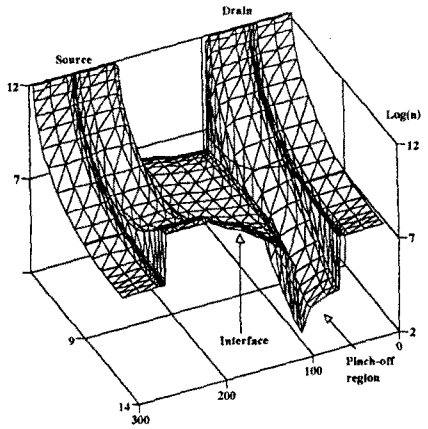

Figure 4 Two-dimensional distribution of mobile electron density in a-Si:H layer under the condition, V_G=5 and V_D=9.6 V (not shown to scale).

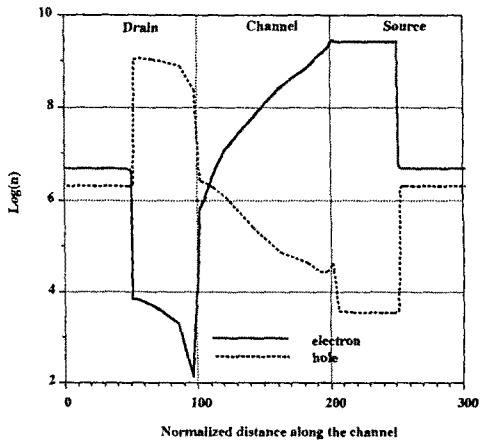

Figure 5 Free electron and hole concentrations along the a-Si:H/insulator interface under V_G=5 V and V_G=9.6 V.

parameters may generate the same I-V characteristics, the optimized parameters used for the I-V simulations are reasonable and the simulation results do demonstrate how TFTSP can be used to analyze transport mechanisms in a-Si:H TFTs. The possibility for the developed program to be refined and used for the optimal modeling and design of a-Si:H TFTs is presented. TFTSP can be employed to further explore device physics in more complicated situation with the accurate physical models for some anomalous characteristics of a-Si:H in TFTs.

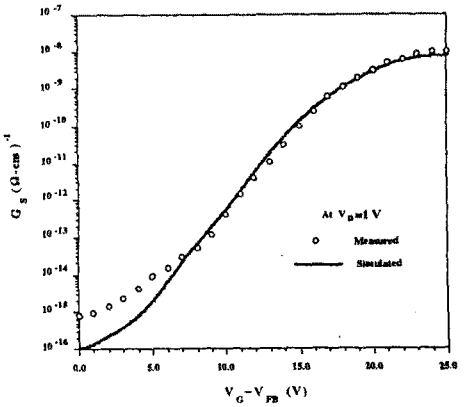

Figure 6 The measured and simulated (semi-logarithmic) transfer characteristics of an a-Si:H TFT at V_D=1 V.

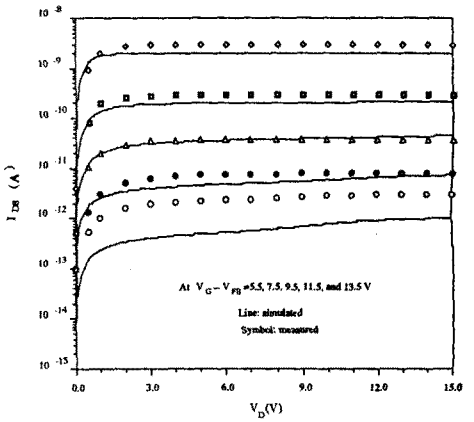

Figure 7 The measured and simulated I-V characteristics of an a-Si:H TFT.

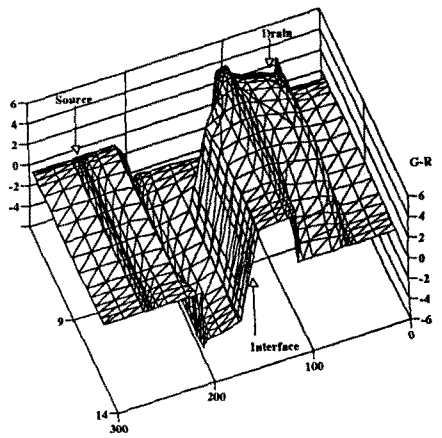

Figure 8 Two-dimensional distribution of generation recombination rate in a-Si:H layer under the condition, V_G=5 and V_D=9.6 V (not shown to scale).

Parameter	description	Value
N_C, N_V (cm^{-3})	effective density of states for the conduction and valence bands	$9.5x10^{20}$
E_G(eV)	mobility / energy band gap	1.72
E_D(eV)	donor energy level below E_C	0.15
E_A (eV)	acceptor energy level above E_V	0.20
	standard deviations of Gaussian distributions of donors	0.06
σ_A (eV)	standard deviations of Gaussian distributions of acceptors	0.04
c_{tn} (cm^2)	capture cross-sections in the conduction band tail for electrons	$5.0x10^{-17}$
c_{td} (cm^2)	capture cross-sections in the conduction band tail for holes	$3.0x10^{-14}$
c_{tn} (cm^2)	capture cross-sections in the valence band tail for electrons	$3.0x10^{-14}$
c_{tp} (cm^2)	capture cross-sections in the valence band tail for holes	$5.0x10^{-17}$
g_{Dtail}($cm^{-3}eV^{-1}$)	density of states of valence band tail at E_V	$2.0x10^{20}$
g_{Atail}($cm^{-3}eV^{-1}$)	density of states of conduction band tail at E_C	$2.0x10^{20}$
E_t (eV)	characteristic energies of conduction band tail	0.027
E_t(eV)	characteristic energies of valence band tail	0.043
N_{DBs} (#/cm^3)	dangling bond state density	$7.5x10^{17}$
E_{D+} (eV)	effective energy level of the $D^+ \leftrightarrow D^0$ transitions	0.59
E_{D-} (eV)	effective energy levels of the $D^- \leftrightarrow D^0$ transitions	1.10
σ_d(eV)	standard deviation of Gaussian distribution of the dangling bond states	0.18
c_{p0} (cm^2)	hole capture cross-sections for $D^0 \rightarrow D^+$	$1.6x10^{-16}$
c_{p-} (cm^2)	hole capture cross-sections for $D^- \rightarrow D^0$	$4.0x10^{-16}$
c_{n+} (cm^2)	electron capture cross-sections for $D^+ \rightarrow D^0$	$2.6x10^{-16}$
c_{n0} (cm^2)	electron capture cross-sections for $D^0 \rightarrow D^-$	$5.4x10^{-17}$

Table 1 Values of important material parameters used for the n-channel a-Si:H TFT simulations.

Parameter	Description	Value
L_{ch} (μm)	channel length	10
L_{ov} (μm)	overlapped drain/source region	50
L_{ex} (μm)	unoverlapped drain/source region	50
W (μm)	channel width	1000
d_{ox} (Å)	insulator thickness	2000
d_{si} (Å)	a-Si layer thickness	3700
K_{ox}	dielectric constant of gate insulator	3.9
K_{si}	dielectric constant of a-Si:H	11.8

Table 2 Values of important device parameters used for the n-channel a-Si:H TFT simulations.

shown in Figure 3 and 4, respectively. The free electron and hole concentrations along the a-Si:H/SiO_2 interface are shown in Figures 5. Note that the pinch-off region is clearly shown at the drain end of the channel. These simulation results represent a self-consistent two-dimensional solution of the transport equations avoiding one-dimensional simplification such as the gradual-channel approximation. Figure 6 shows the corresponding transfer characteristics, which is compared with the experimental data. The conventional threshold voltage (V_T) and field-effect mobility (μ_{FET}) are extracted by assuming that for $V_D << V_G$, $I_D = C_{ox}\mu_{FET}\frac{W}{L}(V_{GS}-V_T-V_D/2)V_D$. The threshold voltage and field-effect mobility can be defined as the intercept less $V_D/2$ and $\mu_{FET} = 1/C_{ox}\frac{L}{W}\frac{dI_D}{dV_G}$, respectively. μ_{FET}=0.08 cm^2/sec-V and V_T-V_{FB}=17.0 V (V_{FB}=-5.5 V) were approximately obtained for the modeled device. Note that the derived value of the field-effect mobility for electron (μ_{FET}=0.08 cm^2/sec-V) is lower than the electron band mobility (μ_n=10 cm^2/sec-V). Figure 7 shows the simulated and measured I-V characteristics for the TFT. There is good agreement between simulation and experiment indicating that these computer simulations are realistic. The net generation/recombination rate under V_G = 5 V, V_D = 9.6 V, and V_S = 0V is illustrated in Figure 8. A graphic representation of this quantity is not straightforward since it may have large values with either sign or steep gradients. The following tranformation [11] was applied:

$$Z = -\,\mathrm{sgn}(G-R)\log\left(1+\frac{|G-R|}{10^{10}\ cm^{-3}sec^{-1}}\right) \qquad (10)$$

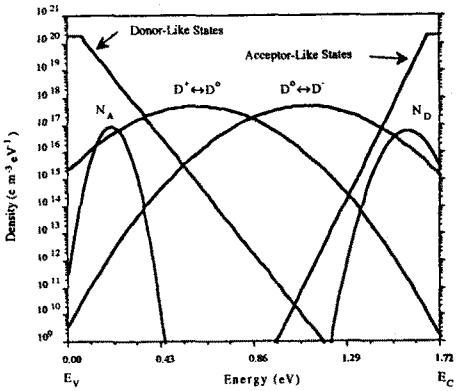

Figure 2 Energy band model for the gap states of a-Si:H.

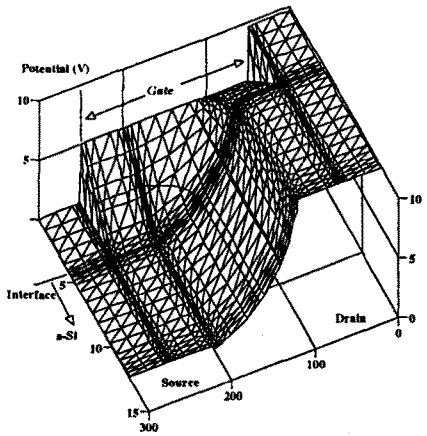

Figure 3 Two-dimensional electrostatic potential distribution when V_G=5 and V_D=9.6 V (not shown to scale).

VII. Summary

A computer program, TFTSP, has been developed for the two-dimensional simulation of a-Si:H TFTs, which provides ability in the choice of physical parameters so that different models can be evaluated and compared. It can handle distributed donor, acceptor, and dangling-bond states, as well as exponential tails. TFTSP was developed to remove as many of the simplifying

REFERNCES

[1]. N. Hirose, Y. Uchida, and M. Matsumura, *Japan. J. Appl. Phys.*, vol. 24, no2, pp. 200-207, February 1985.

[2]. J. G. Shaw and M. Hack, *J. Appl. Phys.*, vol. 65, no. 5, pp. 2124-2129, March 1989.

[3]. J. G. Shaw and M. Hack, *J. Appl. Phys.*, vol. 67, no. 3, pp. 1576-1581, 1 February 1990.

[4]. J. L. Gray, *IEEE Trans. Electron Devices*, vol. ED-36, no. 5, pp. 906-912, 1989.

[5]. J. W. Park, *Ph. D. Dissertation*, Purdue University, 1989.

[6]. C. M. Soukoulis, M. H. Cohen, and E. N. Economou, *Phys. Rev. Lett.*, vol. 53, no.6, pp. 616-619, August 1984.

[7]. W. B. Jackson, S. M. Kelso, C. C. Tsai, J. W. Allen, and S. J. Oh, *Phys. Rev. B*, vol. 31, no. 8, pp. 5187-5198, April 1985.

[8]. G. W. Taylor and J. G. Simmons, *J. Non-Cryst. Solids*, vol. 8-10, pp. 940-946, 1972.

[9]. C. -T. Sah, *Proc. IEEE*, vol. 55, no. 5, May 1967.

[10]. C. -T. Sah and W. Shockley, *Phys. Rev.*, vol. 109, no. 4, 1958.

[11]. S. Selberherr, *Analysis and Simulation of Semiconductor Devices*, Springer-Verlag, 1984.

[12]. C. M. Snowden, *Introduction to Semiconductor Device Modeling*, World Scietific, Singapore, 1986.

[13]. D. L. Scharfetter and H. K. Gummel, *IEEE Trans. Electron Devices*, vol. ED-16, pp. 64-77, January 1969.

[14]. A. de Mari, *Solid-State Electronics*, vol. 11, pp. 33-58, 1968.

[15]. A. D. Sutherland, *Solid-State Electronics*, vol. 23, pp. 1085-1087, 1980.

[16]. G. W. Brown and B. W. Linsay, *Solid-State Electronics*, vol. 19, pp. 991-992, 1976.